Hindawi
Journal of Sensors
Volume 2018, Article ID 3604520, 8 pages
https://doi.org/10.1155/2018/3604520

Research Article

Performance Analysis of Dual-Polarized Massive MIMO System with Human-Care IoT Devices for Cellular Networks

Jun-Ki Hong

Department of Electrical and Electronic Engineering, Youngsan University, Yangsan, Republic of Korea

Correspondence should be addressed to Jun-Ki Hong; jkhong@ysu.ac.kr

Received 24 November 2017; Accepted 18 February 2018; Published 19 April 2018

Academic Editor: Mucheol Kim

The performance analysis of the dual-polarized massive multiple-input multiple-output (MIMO) system with Internet of things (IoT) devices is studied when outdoor human-care IoT devices are connected to a cellular network via a dual-polarized massive MIMO system. The research background of the performance analysis of dual-polarized massive MIMO system with IoT devices is that recently the data usage of outdoor human-care IoT devices has increased. Therefore, the outdoor human-care IoT devices are necessary to connect with 5G cellular networks which can expect 1000 times higher performance compared with 4G cellular networks. Moreover, in order to guarantee the safety of the patient for emergency cases, a human-care Iot device must be connected to cellular networks which offer more stable communication for outdoors compared to short-range communication technologies such as Wi-Fi, Zigbee, and Bluetooth. To analyze the performance of the dual-polarized massive MIMO system for human-care IoT devices, a dual-polarized MIMO spatial channel model (SCM) is proposed which considers depolarization effect between the dual-polarized transmit-antennas and the receive-antennas. The simulation results show that the performance of the dual-polarized massive MIMO system is improved about 16% to 92% for 20 to 150 IoT devices compared to conventional single-polarized massive MIMO system for identical size of the transmit array.

1. Introduction

According to Business Insider, human-care Internet of things (IoT) devices are expected to grow from 120 million in 2015 to 650 million by 2020 [1]. Furthermore, as the use of wearable human-care IoT devices that attach to the body is increasing, the support of a seamless cellular network is essential instead of short-range communication technologies such as Wi-Fi, Zigbee, and Bluetooth. Since human-care IoT devices are closely related to human health and life, seamless communication is very important to guarantee the safety in case of emergencies especially for outdoors.

In addition, the patient can be monitored in real time by cellular networks for both indoors and outdoors when there are various human-care IoT devices connected to the cellular networks. Especially, the connection between cellular networks and human-care IoT devices provides real-time human-care monitoring system via variable human-care services such as ambulance, smartwatch, first aid kit, and a medically equipped smartphone. Further, the collected information of users can be used to prevent accidents via big data analysis. In contrary, short-range communication technologies such as Wi-Fi, Zigbee, and Bluetooth are difficult to communicate from outdoors. In order to guarantee the safety of the users in case of an emergency, it is necessary to connect with a cellular network which provides more stable connection compared to short-range communication technologies for outdoors.

However, the global data usage is expected to increase to 49 exabytes by 2021 [2] as rapid increase in usage of outdoor human-care-related IoT devices. In recent years, more advanced 5G technology and standards are being actively researched to handle the tremendous amount of data from IoT devices [3, 4].

One of the remarkable 5G technology is the massive multiple-input multiple-output (MIMO) system to increase spectral efficiency by a very large number of transmit-antennas. Typically, the transmit-array of a massive MIMO system is composed of tens or hundreds of transmit-antennas to serve tens or hundreds of users simultaneously

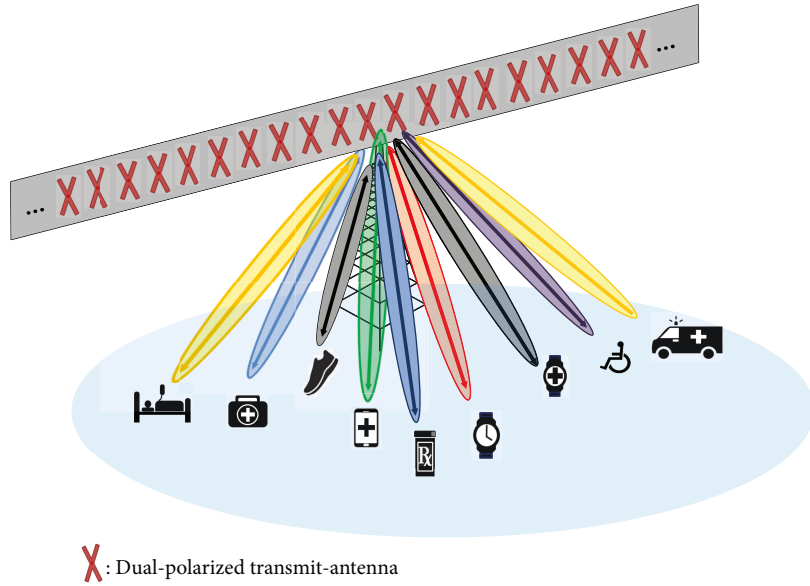

Figure 1: Configuration of the proposed dual-polarized massive MIMO system with various human-care IoT devices for cellular networks.

[5]. Massive MIMO system leads huge improvement in energy efficiency, spectral efficiency robustness, and reliability [6].

A large number of transmit-antenna at a base station (BS) can remarkably improve performance via increasing the multiplexing order to various human-care IoT devices by higher transmit diversity with higher degree of freedoms. In this paper, the performance analysis is achieved when various human-care IoT devices are connected to cellular networks via a dual-polarized massive MIMO system as shown in Figure 1.

To the best of our knowledge, there has not been an analysis that considers the performance between massive the MIMO system and IoT devices for cellular networks. In addition, dual-polarized transmit- and receive-antennas are proposed for BS and IoT device, respectively, to install more antennas and achieve higher performances in limited space.

To evaluate the dual-polarized massive MIMO system, a dual-polarized MIMO spatial channel model (SCM) is proposed which considers the depolarization effects of the dual-polarized antennas. Then, the comparative performance analysis of dual- and single-polarized massive MIMO systems for IoT devices is achieved by system-level simulation.

2. Challenges for Massive MIMO System

Previously, the MIMO system is introduced to increase spectral efficiency by increasing degree of freedoms in space domain by multiple antennas. Afterwards, massive MIMO is introduced to catch up to today's tremendous amount of data traffic with even higher degree of freedoms. However, several issues arise while a large number of transmit-antennas provide more spectral efficiency than conventional MIMO system.

Since transmit-array of massive MIMO is composed of a large number of antennas, the size of the transmit-array will be increased as the number of antenna increases. In other words, the deployment of a large number of transmit-antennas in limited space is very important to implement practical massive MIMO system without unlimited growth of array size.

To deploy a large number of transmit-antennas in limited space, previously, 2 dimensional (2D) planar type of transmitter (Tx) is introduced to reduce the size of the transmit-array [7, 8]. The basic idea of the 2D planar array MIMO system is that the transmit-antennas are installed on a 2D planar grid instead of a 1 dimensional (1D) linear array. Performance comparison between 2D planar and 1D linear transmit-array is analyzed by a function of signal-to-noise ratio (SNR) [7]. 2D planar array performs lower than 1D linear transmit-array because of its higher correlations/interferences between surrounding antennas on the 2D planar array.

Performance analysis of 2D planar and 1D linear transmit-array is conducted by system-level simulations in [7]. Similarly, 2D planar array performs lower than a linear array for same 32 transmit-antennas at the BS. Nevertheless, 2D planar array has several advantages such as reduction of transmit-array size and utilization of vertical beamforming.

3. Dual-Polarized Massive MIMO System

In this paper, a dual-polarized massive MIMO system is proposed which is very effective in reducing the size of a transmit-array by utilization of the extra polarization domain. There are several remarkable advantages for dual-polarized transmit- and receive-antennas since it consists of two colocated orthogonal antennas.

3.1. Advantages of a Dual-Polarized Antenna. One of the major advantages of a dual-polarized transmit-array is the reduction of transmit-array size by half compared to a spatially separate single-polarized transmit-array. Since two colocated orthogonal transmit-antennas are installed on a collocated dual-polarized antenna, a double number of transmit-antennas can be installed compared to a spatially

separate single-polarized transmit-array for identical size of the transmit-array. In other words, the degrees of freedom of a dual-polarized transmit-array can achieve twice the performance compared to a conventional single-polarized transmit-array for identical size of the transmit-array. For example, for a center frequency of 1.9 GHz with a half wavelength, a 64Tx single-polarized transmit-array with a length of 3.67 m can be replaced with 32Tx dual-polarized transmit-array with a length of 1.84 m.

Furthermore, a dual-polarized receive-antenna can be installed at IoT devices to achieve higher performance compared to a single-polarized antenna in identical spaces.

3.2. Utilization of Polarization Domain. Since two independent data streams can be multiplexed at a dual-polarized transmit-antenna, depolarization effect occurs between two data streams. In other words, the extra polarization diversity can be achieved by transmitting two independent data streams from vertically and horizontally polarized antennas at BS. In previous papers, it has been shown that using dual-polarized transmit-antennas can improve performance and reduce transmitter size [9, 10].

However, the performance degradation can occur by polarization mismatch since a single-polarized receive-antenna receives the signal by only one direction and its upper bound of capacity loss from polarization mismatch is 2 bit/s/Hz for multiple dual-polarized antennas and a single-polarized antenna according to [11]. Therefore, the dual-polarized receive-antenna at an IoT device could be the solution to minimize polarization mismatch since vertical and horizontal receive-antenna receives signals at any directions.

Therefore, it is clear that the dual-polarized massive MIMO system is the future for the massive MIMO system to reduce transmit-array size and minimize performance degradation by polarization mismatch. Consequently, the dual-polarized massive MIMO system can be operated by space-polarization division multiple access (SPDMA) which increase spectral efficiency by utilizing both space and polarization domains. The detailed explanations of SPDMA are presented in the next section.

4. SPDMA

The basic idea of SPDMA is increasing spectral efficiency by utilizing both spatial and polarization domains for the dual-polarized MIMO system. In this section, the comparative descriptions of space division multiple access (SDMA), polarization division multiple access (PDMA), and SPDMA techniques are presented.

4.1. SDMA. MIMO system with SDMA is used to extend transmit diversity in the space domain. However, the drawback of the SDMA technique with the single-polarized MIMO system is that the size of a transmit-array increases proportionally as the number of antenna increases. This is one of the major concerns of the massive MIMO system. Moreover, SDMA lacks in utilizing the polarization domain since SDMA only operates for spatially separated single-polarized antennas.

4.2. PDMA. To increase transmit diversity without size expansion, previously, PDMA technique is introduced. The basic idea of PDMA is that the dual-polarized transmit-antenna transmits two independent data streams to different users simultaneously by using orthogonal vertical and horizontal polarizations. The performance analysis between one collocated dual-polarized transmit-antenna and two dual-polarized receive-antennas are provided in [12]. Nevertheless, PDMA lacks spatial diversity at the transmit-array.

4.3. SPDMA. Previous SDMA and PDMA techniques lack polarization and spatial diversity, respectively. In order to overcome these disadvantages, a more advanced SPDMA technique is introduced in [13]. The basic idea of SPDMA is that it increases spectral efficiency by utilizing both space and polarization domains. In other words, the utilization of space domain is achieved by spatially separated dual-polarized antennas and utilization of the polarization domain is achieved by two orthogonal polarizations from vertical and horizontal transmit-antennas. Thus, a one dual-polarized transmit-antenna transmits two different signals simultaneously to different users through the polarization domain. Consequently, the SPDMA technique leads the increment of spectral efficiency not only in space domain but also in polarization domain.

Previously, the comparative performance analysis of the dual- and single-polarized MIMO system is conducted by SDMA and SPDMA techniques via link-level simulation. Simulation results represent the dual-polarized MIMO system with SPDMA achieved higher throughput by extra polarization diversity compared to the single-polarized MIMO with SDMA for identical size of the transmit-array [13]. However, the previous performance analysis of SPDMA is conducted with 8 transmit-antennas which is by a conventional MIMO system. Therefore, previous analysis of the dual-polarized MIMO system with SPDMA is lack of evaluating the performance of a large number of IoT devices.

5. Proposed Dual-Polarized MIMO SCM

3rd Generation Partnership Project (3GPP) MIMO SCM is a geometry-based stochastic model which describes the excess delay, direction of arrival, and direction of departure of multipath for the MIMO channel model [14]. 3GPP MIMO SCM is widely used in modelling the MIMO channels. However, 3GPP MIMO SCM provides a dual-polarized MIMO channel model which considers mixed vertical and horizontal polarizations at a dual-polarized receive-antenna. Thus, previous 3GPP SCM lacks the implementing depolarization effect between vertically and horizontally polarized channels at the dual-polarized receive-antennas which is impossible to consider extra polarization diversity.

Therefore, a dual-polarized MIMO SCM is proposed which considers depolarization effect between dual-polarized transmit- and receive-antennas which operated by the SPDMA technique. Depolarized propagation channels between dual-polarized transmit- and receive-antennas are represented by vertical to vertical (VV), vertical to horizontal

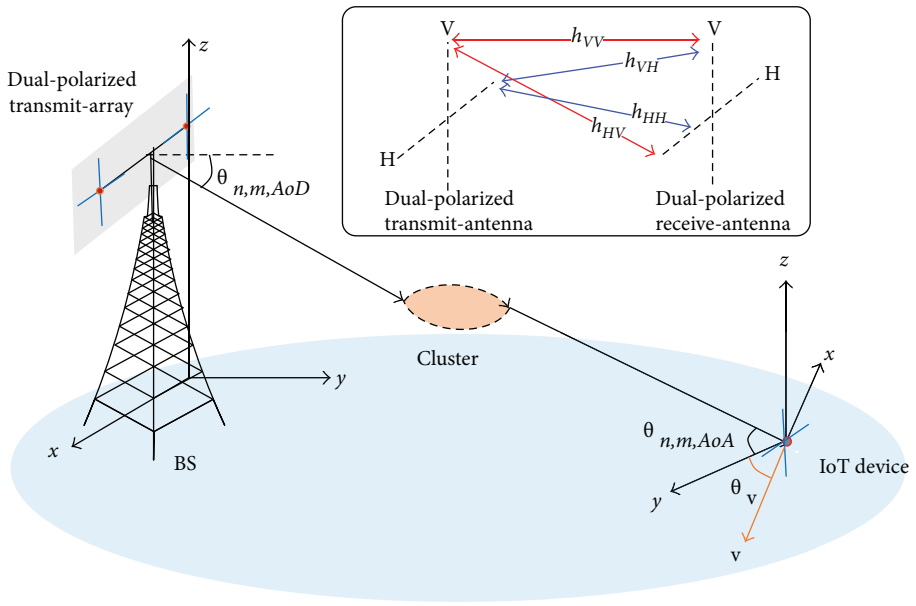

Figure 2: Configuration of the proposed dual-polarized MIMO SCM with an IoT device.

(HV), horizontal to vertical (VH), and horizontal to horizontal (HH) channels as shown in Figure 2.

The proposed dual-polarized MIMO SCM represents BS with S transmit-antenna with S antennas ($S/2 \in N$ of dual-polarized transmit-antennas) and IoT devices with U antennas ($U/2 \in N$ of dual-polarized receive-antennas). Then, (u,s)th dual-polarized MIMO channel component of nth multipath at time t, $\mathbf{H}_{u,s,n}(t)$ can be expressed as

$$\mathbf{H}_{u,s,n}(t) = \sqrt{\frac{P_n \sigma_{SF}}{M}} \sum_{m=1}^{M} \left(\begin{bmatrix} h_{VV} & h_{VH} \\ h_{HV} & h_{HH} \end{bmatrix} \times \exp(\beta_{AoD}) \times \exp(\beta_{\mathrm{AoA}}) \times \exp(\psi_{\mathrm{AoA}}) \right), \tag{1}$$

where

$$\begin{aligned}
h_{VV} &= \chi_{BS,V}(\theta_{n,m,\mathrm{AoD}}) \cdot \left(\sqrt{\frac{\mathrm{XPD}}{1+\mathrm{XPD}}} \exp\left(j\Phi_{n,m}^{(v,v)} \right) \right) \chi_{MS,V}(\theta_{n,m,\mathrm{AoA}}), \\
h_{VH} &= \chi_{BS,H}(\theta_{n,m,\mathrm{AoD}}) \cdot \left(\sqrt{\frac{1}{1+\mathrm{XPD}}} \exp\left(j\Phi_{n,m}^{(v,h)} \right) \right) \chi_{MS,V}(\theta_{n,m,\mathrm{AoA}}), \\
h_{HV} &= \chi_{BS,V}(\theta_{n,m,\mathrm{AoD}}) \cdot \left(\sqrt{\frac{1}{1+\mathrm{XPD}}} \exp\left(j\Phi_{n,m}^{(h,v)} \right) \right) \chi_{MS,H}(\theta_{n,m,\mathrm{AoA}}), \\
h_{HH} &= \chi_{BS,H}(\theta_{n,m,\mathrm{AoD}}) \cdot \left(\sqrt{\frac{\mathrm{XPD}}{1+\mathrm{XPD}}} \exp\left(j\Phi_{n,m}^{(h,h)} \right) \right) \chi_{MS,H}(\theta_{n,m,\mathrm{AoA}}),
\end{aligned} \tag{2}$$

$$\begin{aligned}
\beta_{\mathrm{AoD}} &= j2\pi\lambda^{-1}\{d_s \cos(\theta_{n,m,\mathrm{AoD}})\}, \\
\beta_{\mathrm{AoA}} &= j2\pi\lambda^{-1}\{\cos(\theta_{n,m,\mathrm{AoA}})\}, \\
\psi_{\mathrm{AoA}} &= j2\pi\lambda^{-1}\|v\|[\cos(\theta_{n,m,\mathrm{AoA}} - \theta_{\mathbf{v}})].
\end{aligned}$$

The notations are described in Table 1.

Table 1: Notations of the proposed dual-polarized MIMO SCM.

Notation	Description
P_n	The power of the nth path.
σ_{SF}	The lognormal shadow fading.
M	The number of subpaths per path.
$\theta_{n,m,\mathrm{AoD}}$	Absolute angle of departure (AoD) for the mth subpath of the nth path at the BS with respect to the BS broadside.
$\theta_{n,m,\mathrm{AoA}}$	Absolute angle of arrival (AoA) for the mth subpath of the nth pat at the BS with respect to the BS broadside.
$x_{BS,V}(\theta_{n,m,\mathrm{AoD}})$	The BS antenna complex response for the V-pol. Component.
$x_{BS,H}(\theta_{n,m,\mathrm{AoD}})$	The BS antenna complex response for the H-pol. Component.
$x_{MS,V}(\theta_{n,m,\mathrm{AoA}})$	The antenna complex response for the V-pol. Component of the IoT device.
$x_{MS,H}(\theta_{n,m,\mathrm{AoA}})$	The antenna complex response for the H-pol. Component of the IoT device.
$\Phi_{n,m}^{(x,y)}$	The random phase shift between $V(H)$ of the BS and $V(H)$ component of the IoT device for the mth subpath.
$\|\mathbf{v}\|$	The magnitude of the velocity vector of the IoT device.
$\theta_{\mathbf{v}}$	The azimuth angle of the IoT device velocity vector.
j	Square root of −1.
d_u	The distance from BS antenna element s from the reference ($s = 1$) antenna element in meters. For the reference antenna $s = 1$ where $d_1 = 0$.

Aforementioned, the conventional 3GPP MIMO SCM lacks the implementing depolarization effect between dual-polarized transmit- and receive-antennas. Nevertheless, the

Table 2: Simulation parameters.

Parameter	Assumption
Cellular layout	Hexagonal grid, 19 sites, and 3 sectors per site [15]
Simulation scenarios	Urban macro with AS 8° [14]
Sector radius	350 m
Carrier frequency	1.9 GHz
System bandwidth	10 MHz
Channel estimation	Ideal
XPD	0 and 15 dB
Height of BS	35 m
Height of the IoT device	1.5 m
Antenna spacing	0.5λ
BS transmit power	43 dBm
Signal detection algorithm of the IoT device	MMSE
Average speed of moving IoT devices	3 km/h
Noise figure	7 dB
Path loss	COST 231 Hata model [16]

first channel matrix of the proposed channel coefficient (1) represents separated channel propagations between dual-polarized transmit- and receive-antenna by co- and cross-polarizations; VV, HV, VH, and HH with cross-polarization discrimination (XPD) power imbalance terms.

XPD represents the polarization directivity and the discrimination of the power imbalance between copolarization and cross-polarization components at the dual-polarized receive-antenna. Higher XPD value represents less power leakages between vertically and horizontally polarized channels, and lower XPD value represents more power leakages between vertically and horizontally polarized channels in a dual-polarized receive-antenna. A dual-polarized receive-antenna at IoT device is assumed to receive signals from any directions even IoT devices are randomly oriented.

6. Evaluation Method

6.1. TDD Operation. To achieve system-level simulation, time division duplex (TDD) operation is assumed to exploit channel reciprocity in order to simplify channel state information (CSI) estimation for downlink channel from uplink channel. In this case, the training overhead lineally increases as the number of total IoT devices while the number of transmit-antenna can be extended as large as desired.

6.2. System-Level Simulation and Simulation Parameters. To analyze the performance of the dual-polarized massive MIMO system, both dual- and single-polarized massive MIMO systems are evaluated by 3 sector-based system-level simulation which is conducted from [15]. Also, both vertically and horizontally polarized antenna patterns are modeled with 3 dB beam width of 70° with maximum gain of 17 dBi for 3 sector macro cell scenario. Since the goal of this paper is to analyze the performance between proposed dual- and conventional single-polarized massive MIMO systems for identical size of the transmit-array, assuming that there is no performance degradation due to the battery conditions of the IoT devices. The other important parameters are presented in Table 2.

6.3. Dual-Polarized Receive-Antenna with MMSE Receiver at IoT Devices. As mentioned in Section 3.2, single-polarized receive-antenna receives signal by only one direction which leads to performance degradation by polarization mismatch. However, minimum mean square error (MMSE) receiver enables the IoT device to receive either one of the strongest signals or two signals depending on signal-to-interference-plus-noise ratio (SINR) calculated between two colocated orthogonal receive-antennas since IoT devices are composed of a dual-polarized receive-antenna. In other words, a dual-polarized transmit-antenna at BS is able to serve two orthogonal signals to either one IoT device or more than one IoT devices simultaneously depending on the channel conditions to maximize the performances.

6.4. MRT/Multiple IoT Device Selection Algorithm. In this section, the detailed description of the multi-IoT device selection algorithm is presented. It is assumed that the BS simultaneously transmits data to the S IoT devices that have been optimally selected among the K candidate IoT devices The data symbols for the selected S IoT devices are linearly precoded by maximum ratio transmission (MRT), and transmit signal vector is generated as follows:

$$\mathbf{x} = \mathbf{F}\mathbf{b} = \sum_{k=1}^{S} \mathbf{f}_k b_k, \tag{3}$$

where $\mathbf{F} = [\mathbf{f}_1, \mathbf{f}_2 \cdots \mathbf{f}_S]$ is the $S \times S$ precoding matrix where $\mathbf{f}_k$ is the $S \times 1$ precoding vector for selected kth IoT devices among selected S IoT devices. $\mathbf{b} = [b_1, b_2 \cdots b_S]^T$ is the $S \times 1$ transmit symbol vector where b_k is the transmit symbol for the kth IoT device among the selected S IoT devices.

To mitigate the interference between vertically and horizontally polarized receive-antenna at an IoT device, an MMSE receiver is employed based on perfect CSI. Then, the achievable rate of the kth IoT device with an MMSE receiver can be written as

$$C_k = \log_2\left(1 + b_k^* \mathbf{f}_k^H \mathbf{H}_k^H \left(\mathbf{I} + \sum_{l=1, l\neq k}^{M} \mathbf{H}_k \mathbf{f}_l s_l s_l^* \mathbf{f}_l^H \mathbf{H}_k^H\right)^{-1} \mathbf{H}_k \mathbf{f}_k b_k\right), \tag{4}$$

where $\mathbf{H}_k$ and $\mathbf{I}$ denote $U \times S$ dual-polarized MIMO channel of the kth IoT device and $S \times S$ identity matrix, respectively. The precoding vector for MRT to the kth IoT device is denoted by $\mathbf{f}_k$ obtained as

$$\begin{aligned} \mathbf{f}_k &= \mathbf{V}_k, \\ \mathrm{SVD}[\mathbf{H}_k] &= \mathbf{U}_k \boldsymbol{\Sigma}_k \mathbf{V}_k^H, \end{aligned} \tag{5}$$

where SVD represents the singular value decomposition. $\mathbf{U}_k$, $\boldsymbol{\Sigma}_k$, and $\mathbf{V}_k$ represent $S \times S$ complex unitary matrix, $S \times U$

initialize $G_{opt.} = \{\varnothing\}, C_{\max} = 0, a = 0$
do
$n = \arg\max_{n \in O, n \neq G_{opt.}} \sum_{k \in \{n, G_{opt.}\}} \log_2(1 + \gamma_k)$
$C = \sum_{k \in \{n, G_{opt.}\}} \log_2(1 + \gamma_k)$
if $C > C_{\max.}$.
$G_{opt.} = \{G_{opt.}, n\}$
$R_{\max} = R$
$a = 1$
end
while $a = 1$ **and** $|G_{opt.}| < S_{tx}$

Algorithm 1: Proposed IoT device selection algorithm.

rectangular diagonal matrix, and $U \times U$ complex unitary matrix of the kth IoT device, respectively.

To evaluate the throughput of the proposed massive MIMO systems, the multiuser scheduling algorithm is proposed which serves multiple IoT devices simultaneously with highest IoT-sum-rate by MRT precoding at BS. By MRT, the signals are transmitted by the strongest eigenmodes at BS and the received signals at an IoT device are combined by maximal ratio combining (MRC) technique. The proposed IoT device selection algorithm is specified as follows.where O denotes the universal set of IoTs. S_{tx}, C, and $C_{\max}$ represent the number of transmit-antennas, throughput, and the maximum throughput of the kth IoT device, respectively.

7. Performance Evaluation

7.1. Simulation Scenarios and Level of XPD. To analyze the performance of the proposed dual-polarized MIMO system, three simulation scenarios are proposed: 32Tx dual-polarized massive MIMO system, 32Tx single-polarized massive MIMO system, and 8Tx single-polarized MIMO system. 32Tx single-polarized massive MIMO system represents the identical size of transmit-array of the proposed 32Tx dual-polarized massive MIMO system. Further, 8Tx single-polarized MIMO system represents the reference of conventional MIMO system to compare performance with proposed massive MIMO systems. Moreover, IoT devices are assumed as one dual-polarized receive-antenna to receive signals by any directions.

To investigate the impact of XPD variations on the proposed simulation scenarios, XPD values of 0 and 15 dB are implemented while the proposed dual-polarized MIMO SCM consists XPD terms. XPD = 15 dB is presumed for high level of XPD according to simulation result in [17].

7.2. Performance Analysis. In this subsection, simulation results of the system-level simulation are carried out to analyze the performance of the dual-polarized massive MIMO system compared to single-polarized massive MIMO systems. As mentioned in Subsection 6.4, the performances of the proposed MIMO systems are evaluated by highest sum-rate capacity from the multi-IoT scheduling.

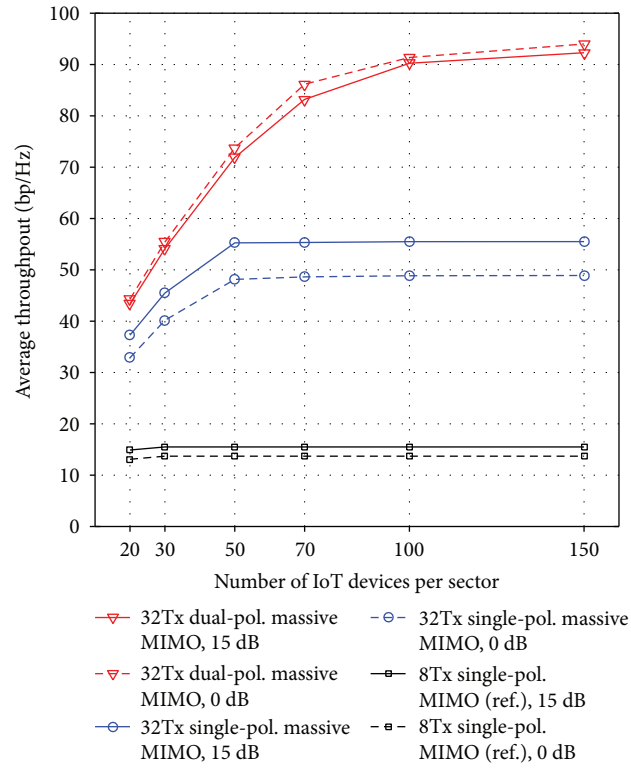

Figure 3: Comparison of the average throughputs.

Figure 3 represents the comparison of the average throughputs between the dual- and single-polarized massive MIMO systems as a function of the number of IoT devices which represents the spectral efficiency. As shown in Figure 3, a proposed 32Tx dual-polarized massive MIMO continuously increases the throughput over 150 IoT devices while a conventional 32Tx single-polarization massive MIMO is impossible to increase the throughputs when more than 50 IoT devices are present in the sector. The performance of the 32Tx dual-polarized massive MIMO system has improved by 16% to 92% for 20 to 150 IoT devices compared to a conventional 32Tx single-polarized massive MIMO system for identical size of the transmit-array.

Furthermore, the average throughput of the dual-polarized massive MIMO for 0 dB is higher than that of the 15 dB because a dual-polarized receive-antenna prefers to receive uncorrelated signals simultaneously instead of selecting one of the strongest signals between two transmitted signals. In other words, completely uncorrelated received signals benefit to increase average sum for the dual-polarized massive MIMO system. Furthermore, the colocated two orthogonal receive-antennas have benefited from uncorrelated channels since less coupling and interferences are generated between two orthogonal receive-antennas. Moreover, the dual-polarized massive MIMO system is insensitive to XPD variations according to throughput gap between XPD = 0 dB and XPD = 15 dB compared to the performance of the single-polarized massive MIMO system.

On the other hand, the single-polarized massive MIMO systems perform higher average throughput for XPD = 15 dB since a higher level of XPD represents the higher directivity

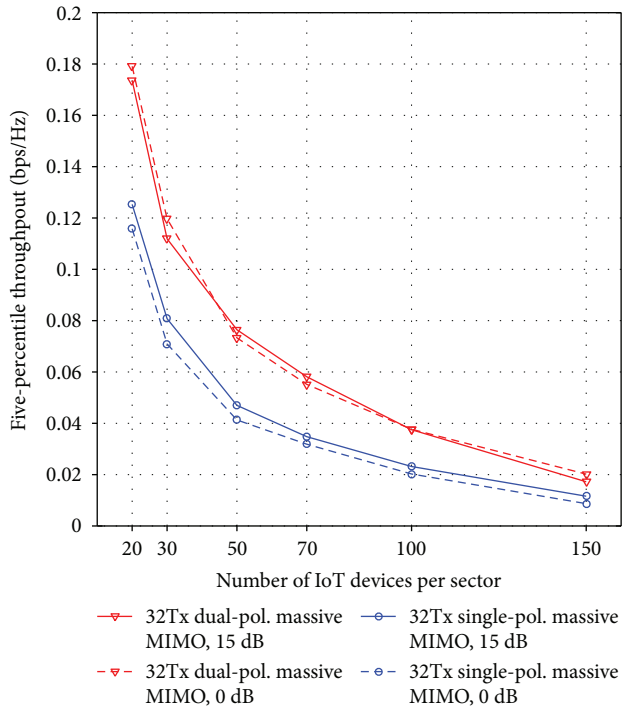

Figure 4: Five-percentile throughputs of the dual- and single-polarized massive MIMO systems.

between transmit and receive antennas. Therefore, transmit-antennas of single-polarized massive MIMO systems have benefited from high XPD since the coupling effect and interference are not generated from colocated transmit-antenna. Since XPD = 0 dB represents the general environment, it is a disadvantage for the single-polarized massive MIMO system.

Further, a conventional 8Tx single-polarized MIMO system is impossible in increasing the performance as the number of IoT devices increases, but the proposed 32Tx dual-polarized massive MIMO system continuously increases the throughput by a higher degree of freedom with the transmit and polarization diversity.

Figure 4 presents the five-percentile (or sector-edge) throughput of the dual- and single-polarized massive MIMO systems. These simulation results indicate that the proposed dual-polarized massive MIMO improves the performance compared to 32Tx single-polarized massive MIMO systems by identical size of the transmit-array.

According to simulation results from Figures 3 and 4, the performance of the dual-polarized massive MIMO system is improved compared to the single-polarized massive MIMO system for identical size of the transmit-array since two colocated polarized transmit-antennas aid to serve more IoT devices via the polarization domain. Consequently, the dual-polarized massive MIMO system benefits from uncorrelated channel environment which is very useful at XPD = 0 dB which represents the general environment.

8. Conclusion

In this paper, the performance between human-care IoT devices and the massive MIMO system is analyzed while massive MIMO system provides seamless communication and big data processing especially for outdoor human-care IoT devices. According to simulation results, the proposed dual-polarized massive MIMO system has several advantages such as reduction of transmit-array size and utilization of polarization domain of the transmit-array. Simulation results show that the performance of the dual-polarized massive MIMO is improved for uncorrelated channel environment for outdoor, XPD = 0 dB. Furthermore, the proposed dual-polarized massive MIMO system doubles the performance compared to the conventional single-polarized massive MIMO system via the identical size of the transmit-array for a large number of IoT devices.

Thus, the proposed dual-polarized massive MIMO system can be the solution to improve performances for outdoor human-care IoT devices while dual-polarized massive MIMO systems enable in reducing the sizes of the transmitters and receivers.

Conflicts of Interest

The author declares that he has no conflicts of interest.

References

[1] Business Insider, *Internet of Things in Healthcare: Information Technology in Health*, December 2016, http://www.businessinsider.com/internet-of-things-in-healthcare-2016-8.

[2] Cisco, *Cisco Visual Networking Index: Global Mobile Data Traffic Forecast Update, 2014–2019*, http://www.cisco.com/c/en/us/solutions/collateral/service-provider/visual-networking-index-vni/white_paper_c11-520862.pdf.

[3] M. R. Palattella, M. Dohler, A. Grieco et al., "Internet of things in the 5G era: enablers, architecture, and business models," *IEEE Journal on Selected Areas in Communications*, vol. 34, no. 3, pp. 510–527, 2016.

[4] G. A. Akpakwu, B. J. Silva, G. P. Hancke, and A. M. Abu-Mahfouz, "A survey on 5G networks for the internet of things: communication technologies and challenges," *IEEE Access*, vol. PP, no. 99, p. 1, 2017.

[5] T. Marzetta, "Noncooperative cellular wireless with unlimited numbers of base station antennas," *IEEE Transactions on Wireless Communications*, vol. 9, no. 11, pp. 3590–3600, 2010.

[6] E. Larsson, O. Edfors, F. Tufvesson, and T. Marzetta, "Massive MIMO for next generation wireless systems," *IEEE Communications Magazine*, vol. 52, no. 2, pp. 186–195, 2014.

[7] J.-K. Hong, H. Joung, H.-S. Jo, C. Mun, and J.-G. Yook, "A three dimensional model for dual polarized MIMO channel of the planar array antennas," *International Journal of Smart Home*, vol. 7, no. 1, 2013.

[8] Y.-H. Nam, B. Ng, K. Sayana et al., "Full-dimension MIMO (FD-MIMO) for next generation cellular technology," *IEEE Communications Magazine*, vol. 51, no. 6, pp. 172–179, 2013.

[9] J. Jootar, J.-F. Diouris, and J. R. Zeidler, "Performance of polarization diversity in correlated Nakagami-m fading channels," *IEEE Transactions on Vehicular Technology*, vol. 55, no. 1, pp. 128–136, 2006.

[10] R. U. Nabar, H. Bolcskei, V. Erceg, D. Gesbert, and A. J. Paulraj, "Performance of multiantenna signaling techniques in the presence of polarization diversity," *IEEE Transactions on Signal Processing*, vol. 50, no. 10, pp. 2553–2562, 2002.

[11] H. Joung, H.-S. Jo, C. Mun, and J.-G. Yook, "Capacity loss due to polarization-mismatch and space-correlation on MISO channel," *IEEE Transactions on Wireless Communications*, vol. 13, no. 4, pp. 2124–2136, 2014.

[12] S.-C. Kwon and G. L. Stuber, "Polarization division multiple access on NLoS wide-band wireless fading channels," *IEEE Transactions on Wireless Communications*, vol. 13, no. 7, pp. 3726–3737, 2014.

[13] H. Joung, H.-S. Jo, C. Mun, and J.-G. Yook, "Space-polarization division multiple access system with limited feedback," *KSII Transactions on Internet and Information Systems*, vol. 8, no. 4, pp. 1292–1306, 2014.

[14] 3GPP TR 25.996 V14.0.0, "Spatial channel model for multiple input multiple output (MIMO) simulations," Tech. Rep., 2017, http://www.etsi.org/deliver/etsi_tr/125900_125999/125996/14.00.00_60/tr_125996v140000p.pdf.

[15] R. Srinivasan, Ed., *IEEE 802.16m Evaluation Methodology Document (EMD)*, 2008, http://ieee802.org/16/tgm/docs/80216m-08_004r2.pdf.

[16] E. Damosso, L. M. Correia, and European Commission, "COST Action 231: Digital mobile radio towards future generation systems: final report," 1999, http://www.lx.it.pt/cost231/final_report.htm.

[17] J.-U. Jeong, J.-H. Kim, and C. Mun, "Analysis of massive MIMO wireless channel characteristics," *The Journal of Korea Information and Communications Society*, vol. 38B, no. 3, pp. 216–221, 2013.